IEEE Access
Multidisciplinary | Rapid Review | Open Access Journal

Received May 12, 2020, accepted June 14, 2020, date of publication June 22, 2020, date of current version July 1, 2020.

Digital Object Identifier 10.1109/ACCESS.2020.3004154

Coherent Polarization States Multiplexer and Its Feasibility in Quantum Communication

WEIZHAO LU AND JIANFENG QIU
[1]Medical Engineering and Technical Center, Shandong First Medical University and Shandong Academy of Medical Sciences, Tai'an 271016, China
[2]Department of Radiology, Shandong First Medical University and Shandong Academy of Medical Sciences, Tai'an 271016, China

Corresponding author: Jianfeng Qiu (jfqiu100@gmail.com)

This work was supported in part by the National Key Research and Development Program of China under Grant 2016YFC0103400, in part by the Key Research and Development Program of Shandong Province under Grant 2017GGX201010, in part by the Taishan Scholars Program of Shandong Province under Grant TS201712065, and in part by the Academic Promotion Programme of Shandong First Medical University under Grant 2019QL009.

ABSTRACT In this paper, a multiplexing technique of coherent polarization states based on three-dimensional rotation group is proposed. The technique applies two Stokes parameters in one polarized light as signal and local oscillator (LO), and combines them in the single spatial mode. Three-dimensional rotation group SO(3) is used to describe the transformation of Stokes parameters. SO(3) is decomposed into three subgroups, with each subgroup represents a rotation along different axes. A multiplexer is designed with three electro-optical crystals to realize the function of three-dimensional rotation group. The multiplexer achieves an ergodicity of polarization states. Signal and LO propagates in the same spatial mode, multiplexing of polarization states is realized. Finally, the multiplexer is tested in a free space quantum communication system and its feasibility in quantum communication is confirmed.

INDEX TERMS Optical polarization, stokes parameters, quantum cryptography, optical communication equipment.

I. INTRODUCTION

The world's first quantum key distribution (QKD) demonstration in free space was performed in 1996 [1]. By now, tremendous progresses have been made in this field, many prepare-and-measurement systems have been proposed [2], [3]. Most of them were based on discrete-variable (DV) [2], [4]–[6] or entangled state [7], [8], which had poor practicability due to rare light source and expensive single photon detector. Continuous-variable QKD (CV-QKD), as one of the implementation schemes of QKD, possesses several advantages over DV-QKD: easier implementation [9]–[11] and lower cost [12]–[14], etc. Most of the CV-QKD systems were performed while splitting signal and LO as Mach-Zehnder interferometer's two arms [15]–[17]. Atmospheric scattering adds difficulty to synchronization of the two beams in free space, and it's also hard for an accurate interference of them at Bob's side. Although Huang *et al.* proposed a locally LO scheme [18], [19], it still required precise secure phase compensations. To overcome the fore-mentioned issues, Lorenz *et al.* proposed a polarization encoding theory which multiplexed signal and LO in one spatial mode [20], Elser *et al.* presented a free space CV-QKD system with multiplexing of coherent polarization states using electro-optical modulator (EOM) and magneto-optic modulator (MOM) [21], Heim *et al.* improved Elser's system by using two EOMs associated with a half wave plate (HWP) to implement multiplexing [22], [23].

Besides polarization encoding, multiplexing of polarization were also widely used in other fields. Hockett *et al.* conducted photoionization experiments with polarization multiplexing [24], Grassi *et al.* presented a centralized light source optical access network based on polarization multiplexing [25], several groups used multiplexing of polarization to assist orbital angular momentum modulation [26], [27] or enhance channel capacity [28].

In this paper, we proposed a polarization multiplexing technique based on rotation group SO(3), used two quadratures of Stokes parameters as signal and LO in CV-QKD, and allowed co-propagation of signal and LO in one polarized light beam. Self-made coherent polarization states multiplexer, which possessed the ability of SO(3) transformation, was employed

The associate editor coordinating the review of this manuscript and approving it for publication was Xinxing Zhou.

to implement polarization multiplexing. The multiplexer was tested in an experimental setup to prove its feasibility and application in free space QKD.

II. POLARIZATION AND ELECTRO-OPTICAL CRYSTAL

A. POLARIZATION CHARACTERIZATION

Polarization, as a characteristic of light wave, could be described by complex-number representation, Jones Vector, Poincaré Sphere, etc [20]. In 1852, Stokes firstly described polarization states by light intensity $\{S_0, S_1, S_2, S_3\}$, also known as the Stokes parameters [21]. These parameters could be acquired by measuring the intensity of light, and its three polarization components $\{S_1, S_2, S_3\}$ could be mapped to one fixed point on the Poincaré Sphere, as shown in Figure 1.

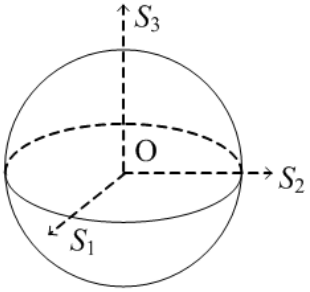

FIGURE 1. Poincaré sphere with stokes parameters S_1, S_2 and S_3.

It is known that the above Stokes operators obey the Lie algebra of SU(2) [29],

$$\begin{cases} [\hat{S}_i, \hat{S}_j] = 2i \in_{ijk}, i, j, k = 1, 2, 3 \\ [\hat{S}_0, \hat{S}_j] = 0, i = 1, 2, 3 \\ \hat{S}_0(\hat{S}_0 + 2) = \hat{S}_1^2 + \hat{S}_2^2 + \hat{S}_3^2 \end{cases} \tag{1}$$

The connection between Stokes operators and SU(2) algebra is very useful in polarization spin [29]. In this paper, we used rotation group SO(3) to describe polarization rotation, which is a subgroup of SU(2). Also in Eq.(1), it could be seen that the three Stokes operators $\{\hat{S}_1, \hat{S}_2, \hat{S}_3\}$ satisfy canonical commutation relation. According to the Heisenberg uncertainty principle, we have

$$(\Delta\hat{S}_i)(\Delta\hat{S}_j) \geq \left|\left\langle \hat{S}_k \right\rangle\right|, \quad i, j, k = 1, 2, 3 \tag{2}$$

Eq.(2) indicates that precision of simultaneous measurement of a pair of Stokes parameters is limited by the uncertainty principle. In this study, we chose S_2 and S_3 of Stokes parameters of the same beam as signal and LO. This technique is also known as polarization multiplexing [20]–[23].

B. ELECTRO-OPTICAL CRYSTALS

When electrical field is added to an electro-optical crystal, charge transfer and micro structural deformation will happen inside the crystal. These alterations lead to a change of refractive index, which is known as electro-optical effect [30]. When light beams pass through such an electro-optical crystal, the change of refractive index leads to a phase retardation in different directions, and polarization states change as well. In this study, $LiNbO_3$ was selected as the electro-optical crystal, which had a linear electro-optical effect also known as the Pockels effect [31]. $LiNbO_3$ has a crystal symmetry of 3m, the change in refractive index due to an electrical field could be expressed by

$$\Delta(1/n^2)_i = \sum r_{ij} E_i, \quad i = 1, ...6, \ j = 1, ...3 \tag{3}$$

where n is the refractive index, r_{ij} is the electrical-optical coefficients, E_x, E_y and E_z represent electrical fields from corresponding directions. Define c-axis cutting crystal as Z-type crystal, according to Pockels effect and Eq.(3), when an X-directional (a-axis) electrical field is added to the Z-type crystal, phase retardation due to X-directional (a-axis) electrical field could be obtained,

$$\delta_Z = \frac{2\pi n_o^3 r_{22}}{\lambda} \frac{l}{d} V_X \tag{4}$$

Similarly, for a a-axis cutting X-type crystal, phase retardation due to X-directional (c-axis) electrical field could be written as:

$$\delta_X = \frac{2\pi l}{\lambda}(n_o - n_e) + \frac{\pi(n_e^3 r_{33} - n_o^3 r_{13})}{\lambda} \frac{l}{d} V_Z \tag{5}$$

where n_o and n_e are the ordinary and extraordinary refractive indices, l and d are length and width of the crystal. V_X and V_Z are driving voltages of X-type and Z-type crystals. Eq.(4) and (5) indicated that phase retardation was proportional to driving voltage V, so through controlling of driving voltage V, we could alter phase retardation of the crystal.

III. DESIGN OF THE SO(3) TRANSFORMATION MULTIPLEXER FOR COHERENT POLARIZATION STATES MULTIPLEXING

A. SO(3) TRANSFORMATION

For crystals whose angle between principal optical axis and horizontal plane is known, its Muller matrix could be obtained according to matrix optics [32]. Here we used three dimensional rotation group SO(3) which was a three-order sub-matrix of Muller matrix, to represent Muller matrix. SO(3) matrix of X- and Z-type crystal could be expressed as follows:

$$M_X = \begin{bmatrix} 1 & 0 & 0 \\ 0 & \cos\delta_X & \sin\delta_X \\ 0 & -\sin\delta_X & \cos\delta_X \end{bmatrix}$$
$$M_Z = \begin{bmatrix} \cos\delta_Z & 0 & -\sin\delta_Z \\ 0 & 1 & 0 \\ \sin\delta_Z & 0 & \cos\delta_Z \end{bmatrix} \tag{6}$$

where δ is phase retardation, and according to Eq.(4) and (5), it relates to the driving voltage. Here we have two types of SO(3) matrix, namely M_X and M_Z. According to the Lie algebra of SO(3), M_X is a rotation group rotating polarization states along OS_1 axis in Poincaré Sphere, and M_Z rotates polarization states along OS_2, as indicated in Figure 2.

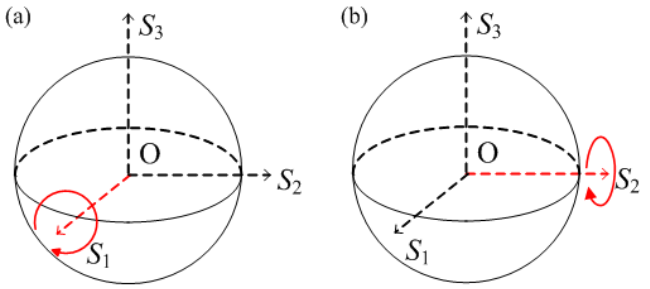

FIGURE 2. Rotation directions for $LiNbO_3$ crystals. (a) *X*-type crystal, (b) *Z*-type crystal.

B. DESIGN OF THE MULTIPLEXER

With the above SO(3) matrix, we could now configure polarization states multiplexer. When we combine *X*-type and *Z*-type crystals to form a multiplexer, based on matrix optics, the output S_{out} polarization states could be calculated by

$$\begin{aligned}&\begin{bmatrix} S_{out,1} & S_{out,2} & S_{out,3} \end{bmatrix}^T \\ &= M_Z \cdot M_X \cdot \begin{bmatrix} S_{in,1} & S_{in,2} & S_{in,3} \end{bmatrix}^T \\ &= \begin{bmatrix} \mathrm{S_{in,1}}\cos\delta_Z + S_{in,2}\sin\delta_X \sin\delta_Z - S_{in,3}\cos\delta_X \sin\delta_Z \\ S_{in,2}\cos\delta_X + S_{in,3}\sin\delta_X \\ S_{in,1}\sin\delta_Z - S_{in,2}\cdot\sin\delta_X\cos\delta_Z + S_{in,3}\cos\delta_X\cos\delta_Z \end{bmatrix}\end{aligned} \tag{7}$$

Consider an arbitrary incident polarization state S_{in} with Stokes parameters $[S_{\text{in},1}, S_{\text{in},2}, S_{\text{in},3}] = [-0.3, -0.5, 0.8124]$. When δ_X and δ_Z range from $[-\pi, \pi]$, all possibilities of S_{out} could be calculated using Eq.(7). And Figure 3 gives a map of all the possible S_{out} on the Poincaré Sphere. In Figure 3, the star mark represents the incident coherent polarization state, and red dots means all the possible output states. As indicated in Figure 3b and 3c, there exists a blank area on the surface of the sphere, which means neither *X*-*Z* type encoder nor *Z*-*X* type multiplexer could achieve an ergodicity on the Poincaré Sphere. So we could draw a conclusion that two SO(3) sub-groups could not achieve arbitrary polarization state transformation.

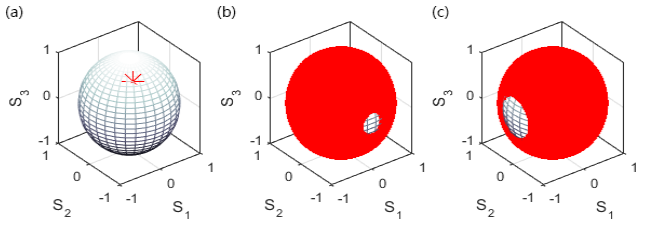

FIGURE 3. The incident coherent polarization state S_{in} and all possibilities of S_{out} on Poincaré Sphere for two SO(3) matrices' situation. (a) Incident coherent state S_{in}, (b) all possibilities of S_{out} of X-Z type multiplexer, (c) all possibilities of S_{out} of Z-X type multiplexer.

Let's consider using three SO(3) sub-groups, *X*-*Z*-*X* or *Z*-*X*-*Z*. Considering *X*-*Z*-*X* combination, according to matrix optics, the output polarization state S_{out} could be calculated by

$$\begin{aligned}&\begin{bmatrix} S_{out,1} & S_{out,2} & S_{out,3} \end{bmatrix}^T \\ &= M_{X3} \cdot M_{Z2} \cdot M_{X1} \cdot \begin{bmatrix} S_{in,1} & S_{in,2} & S_{in,3} \end{bmatrix}^T \\ &= \begin{bmatrix} A_{11} & A_{12} & A_{13} \\ A_{21} & A_{22} & A_{23} \\ A_{31} & A_{32} & A_{33} \end{bmatrix} \cdot \begin{bmatrix} S_{in,1} & S_{in,2} & S_{in,3} \end{bmatrix}^T\end{aligned} \tag{8}$$

where A_{ij} could be calculated by

$$\begin{bmatrix} A_{11} \\ A_{12} \\ A_{13} \\ A_{21} \\ A_{22} \\ A_{23} \\ A_{31} \\ A_{32} \\ A_{33} \end{bmatrix} = \begin{bmatrix} \cos\delta_{Z,2} \\ \sin\delta_{X,3}\cdot\sin\delta_{Z,2} \\ -\cos\delta_{X,1}\cdot\sin\delta_{Z,2} \\ \sin\delta_{X,3}\cdot\sin\delta_{Z,2} \\ \cos\delta_{X,3}\cdot\cos\delta_{X,1} - \sin\delta_{X,3}\cdot\cos\delta_{Z,2}\cdot\sin\delta_{X,1} \\ \cos\delta_{X,3}\cdot\sin\delta_{X,1} + \sin\delta_{X,3}\cdot\cos\delta_{Z,2}\cdot\cos\delta_{X,1} \\ \cos\delta_{X,3}\cdot\sin\delta_{Z,2} \\ -\sin\delta_{X,3}\cdot\cos\delta_{X,3} - \cos\delta_{X,3}\cdot\cos\delta_{Z,2}\cdot\sin\delta_{X,3} \\ \sin\delta_{X,3}\cdot\sin\delta_{X,1} - \cos\delta_{X,3}\cdot\cos\delta_{Z,2}\cdot\cos\delta_{X,1} \end{bmatrix} \tag{9}$$

We took the same arbitrary incident polarization state $S_{in} = [-0.3, -0.5, 0.8124]$, and made $\delta_{X,1}$ and $\delta_{Z,2}$ ranging from $[-\pi, \pi]$ to give a simulation of all the possible S_{out} onto the Poincaré Sphere using Eq.(8) and (9) as shown in Figure 4.

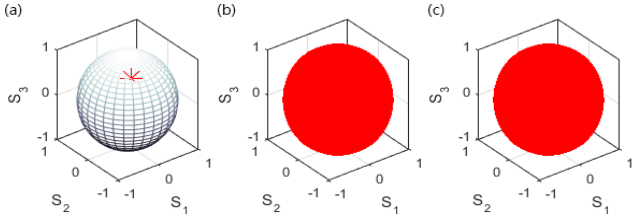

FIGURE 4. The incident coherent polarization state S_{in} and all possibilities of S_{out} on Poincaré Sphere for three SO(3) matrices' situation. (a) Incident coherent state S_{in}, (b) all possibilities of S_{out} of X-Z-X type multiplexer, (c) all possibilities of S_{out} of Z-X-Z type multiplexer.

As shown in the above figure, both *X*-*Z*-*X* and *Z*-*X*-*Z* type could achieve an ergodicity on Poincaré Sphere, that is to say, three SO(3) sub-groups could realize arbitrary polarization states transformation. In our experiment, we prepared a $-45°$ linear polarized state as the incident state, which was on the negative half of OS_2 axis, a *Z*-type SO(3) matrix at the beginning of the matrix array was not working. Therefore, we chose *X*-*Z*-*X* SO(3) matrix array as our multiplexer. Combine Eq.(4), (5) and (8), we could build the connection

between driving voltage V and the output polarization states. In other words, changing the voltage leads to the change of polarization states.

C. MULTIPLEXING OF COHERENT POLARIZATION STATES

As mentioned above, in our experimental configuration, a $-45°$ linear polarized beam (Stokes parameters $[1, 0, -1, 0]$) was prepared as the incident state of the SO(3) transformation multiplexer. According to Eq.(8) and (9), we have

$$\begin{cases} S_{out,1} = -\sin\delta_{Z,2}\sin\delta_{X,1} \\ S_{out,2} = -\cos\delta_{X,3}\cos\delta_{X,1} + \sin\delta_{X,3}\cos\delta_{Z,2}\sin\delta_{X,1} \\ S_{out,3} = \sin\delta_{X,3}\cos\delta_{X,1} + \cos\delta_{X,3}\cos\delta_{Z,2}\sin\delta_{X,1} \end{cases} \quad (10)$$

As mentioned in Sec II, S_2 and S_3 was selected as signal or LO, S_1 remained the same during multiplexing process, so for simplification, we defined $\sin\delta_{Z,2} \approx 0$, so $\cos\delta_{Z,2} \approx 1$. As the first and third SO(3) matrix were the same type of crystals, we simply added same driving voltage to these to crystals, leading to the same phase retardation $\delta_{X,1} = \delta_{X,3}$. Then Eq.(10) could be simplified as:

$$\begin{cases} S_{out,2} = -\cos\delta_{X,3}\cos\delta_{X,1} + \sin\delta_{X,3}\sin\delta_{X,1} = -\cos 2\delta_{X,1} \\ S_{out,3} = \sin\delta_{X,3}\cos\delta_{X,1} + \cos\delta_{X,3}\sin\delta_{X,1} = \sin 2\delta_{X,1} \end{cases} \quad (11)$$

Here $S_{out,1}$ was very small. Eq.(11) shows when S_2 is chosen as signal and S_3 is selected as LO, S_2 is the smaller one with greater variation, and S_3 is the larger one with rather smaller variation. Mapping onto Poincaré Sphere, the encoding zone is around the north pole (See Figure 5a). Similarly, when S_3 is chosen as signal, the encoding zone is around the eastern end (See Figure 5b). It could be seen that the Stokes parameters S_2 and S_3 satisfy the signal and LO's requirement of CV-QKD. S_2 and S_3 from the same coherent state belong to one spatial mode. Using SO(3) transformation, signal and LO of the coherent polarization states propagate in a single spatial mode under our experimental setup, and at the same time the signal is encoded, this is the so-called multiplexing of coherent polarization states or polarization multiplexing.

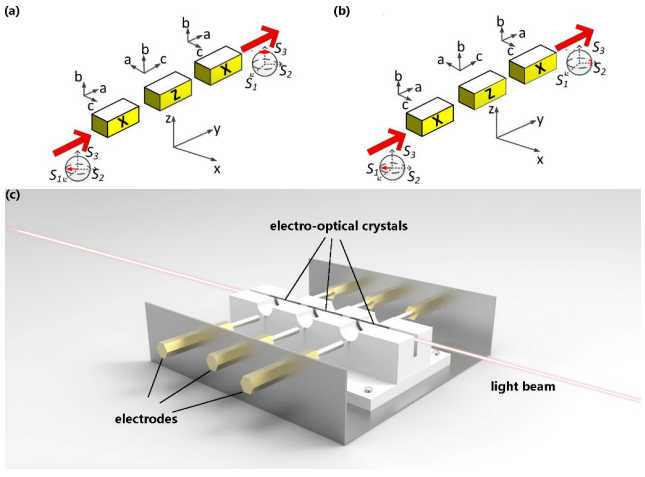

FIGURE 5. Multiplexing of coherent polarization states based on SO(3) transformation. (a) Encoding process of S_2. (b) Encoding process of S_3. The red arrow represents incident polarization state, and the red area means encoding area. The upper coordinates are crystal axes, and the lower are the actual coordinates of our experiment. (c) 3-D view of the coherent polarization states multiplexer.

D. APPLICATION IN OPTICAL COMMUNICATION SYSTEM

To test the performance of SO(3) transformation multiplexer, we configured an optical communication system which contained three parts: linear polarization state preparation module, polarization multiplexing module and receiving module. The experimental setup is shown in Figure 6.

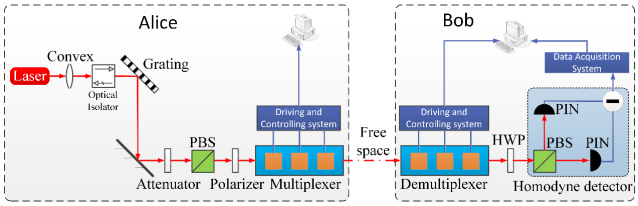

FIGURE 6. The experimental setup. PBS represents polarization beam splitter.

(1) Linear polarization state preparation module. An 808nm continuous beam is emitted by a semiconductor laser source, followed by a convex to get an ideal parallel light. An optical isolator is used to prevent the laser source from reflection. After a spatial filtering grating, a beam of monochromatic coherent light is obtained. Variable optical attenuation (VOA) has an attenuation range from 2% to 100%. A Wollaston prism is used as PBS to split the incident beam into two linear polarized beams, and the horizontal one is reserved. Via a polarizer, a near $-45°$ linear polarized light (Stokes parameters $[1, 0, -1, 0]$) is obtained.

(2) Polarization multiplexing module. Polarization multiplexing module is made up of PC, high-voltage driving circuit and SO(3) transformation multiplexer. High voltage driving circuit which is controlled by an ARM chip, provides corresponding voltage to the multiplexer. The multiplexing process works as follows. Firstly, ARM randomly selects signal and LO from S_2 and S_3, and uses Gaussian random number as modulating signal, the circuit drives the multiplexer with corresponding voltage, and modulated signal is sent to PC via USB port simultaneously. When the prepared linear polarized light passes through the multiplexer, the signal with S_2 or S_3 modulated is obtained. And the signal and LO are sent to receiving module via free space. The communication system was only an experimental setup, the distance between Alice and Bob was only 1 m, so the influence of atmospheric turbulence could be neglected.

(3) Receiving module. The receiving module consists of two parts, namely, a demultiplexer and an HWP. The demultiplexer has the same structure as the multiplexer. Let the incident beam at Bob's side be $P_{in} = (S'_{in,0}, S'_{\text{in},1}, S'_{in,2}, S'_{in,3})^T$, we apply the same voltage to the first and third X-type crystal, which leads to the same phase retardation and the

same SO(3) matrix of these two crystals. The demultiplexing process could be expressed by $[S'_{out,1}, S'_{out,2}, S'_{out,3}]^T = H_{1/2} \cdot M_X \cdot M_Z \cdot M_X \cdot [S'_{in,1}, S'_{in,2}, S'_{in,3}]^T$. Combined with Eq.(10), we have

$$S'_{out,1} = AS'_{in,1} + BS'_{in,2} + CS'_{in,3} \tag{12}$$

where $A = \sin\delta'_{X,1}\sin\delta'_{Z,2}$, $B = \cos^2\delta'_{X,1} - \sin^2\delta'_{X,1}\cos\delta'_{Z,2}$, and $C = \sin\delta'_{X,1}\cos\delta'_{X,1}(1+\cos\delta'_{Z,2})$ ($\delta'_{X,1} = \delta'_{X,3}$). This implies that we could select measurement basis by changing the driving voltage of the demultiplexer. Specifically, we could make A = 0, B = −1, C = 0 to measure S_2, and A = 0, B = 0, C = 1 to measure S_3.

After randomly choosing measurement basis by changing the driving voltage of the demultiplexer, the light is split by PBS into the homodyne detector. After demultiplexing and homodyne detection, the light sent by Alice is measured by either S_2 or S_3. DAQ PCI6111E is applied to acquire the voltage, and the data is finally sent to PC at Bob's side.

In the experimental setup, channel noise, measurement noise and other kind of noise produce a tremendous influence on coherent detection, so an efficient signal identification method should be applied in order to distinguish the quantum state correctly. In this study, we used the recurrent quantum neural network (RQNN) with Schrödinger equation for system control and coherent states extraction [33].

The RQNN algorithm runs as follows: In Schrödinger equation, $f(x,t) = |\psi(x,t)|^2$ is probability density function (PDF). Define the output of RQNN as $\hat{y} = \int x(t)\cdot f(x,t)dx$, we have the Schrödinger equation which describes the RQNN model [33].

$$i\hbar\frac{\partial\psi(x,t)}{\partial t} = -\frac{\hbar^2}{2m}\nabla^2\psi(x,t) + \zeta W\left(y_a(t) + e(t) - \hat{y}\right)\phi(x,t)\psi(x,t) \tag{13}$$

where $\zeta W\left(y_a(t)+e(t)-\hat{y}\right)\phi(x,t)$ is the spatial potential energy $V(x,t)$, $y_a(t)+e(t)$ is the input signal, $y_a(t)$ is the actual signal and $e(t)$ is the unknown noise. $W\left(y_a(t)+e(t)-\hat{y}\right)$ is the weight, which is also a function of the input and output of the signal. When the input signal stimulates RQNN neurons to let the RQNN establish a spatial potential energy, according to Eq.(12), the quantum state $\psi(x,t)$, which represents the collective response of the neurons, evolves with the potential energy. By establishment of the potential energy through RQNN, coherent states could be accurately extracted from the noise [33].

IV. RESULTS AND DISCUSSIONS

A. MULTIPLEXING VERIFICATION OF THE MULTIPLEXER

To test multiplexing function of the self-made multiplexer, Thorlabs's polarimeter PAX5710IR1-T was applied for polarization measurement and the result was sent to computer. S_2 or S_3 was randomly selected as signal, and according to Eq.(4) (5) and (11), relevant driving voltages were calculated and added to the multiplexer. Via the polarimeter, the resulting polarization states were mapped onto Poincaré Sphere as illustrated in Figure 7.

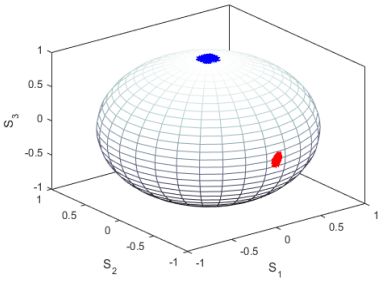

FIGURE 7. Multiplexing results of the multiplexer, the red area is the polarization states when encoding S_3, and the blue area is the polarization states when encoding S_2.

As indicated in Figure 7, multiplexing results were consistent with theoretical design in Section III, the blue and red area accorded well with the area in Figure 5. That is to say, when S_2 is selected as weak signal, and S_3 is selected as strong LO, the encoding is in the blue area. Signal and LO propagates in the same spatial mode, which not only meets the security requirement of CV-QKD, but also fulfill the multiplexing of signal and LO. It is the same situation when S_3 is selected as weak signal, and S_2 is selected as strong LO.

B. PERFORMANCE VERIFICATION OF THE MULTIPLEXER

For performance verification of the multiplexer, S_2 was selected as signal and S_3 was selected as LO at Alice's side. At Bob's side, S_2 was selected as measurement base. The power of light beam incident to the multiplexer was 1mW. 16-bit Gaussian random number was selected as modulating signal for S_2. Driving voltage of the multiplexer and demultiplexer was calculated and added to the devices via driving and controlling system. The sending and receiving signal is displayed in Figure 8. It could be seen that the waveforms of sending and receiving data were almost the same, and there was little noise in the receiving data. After quantization of the

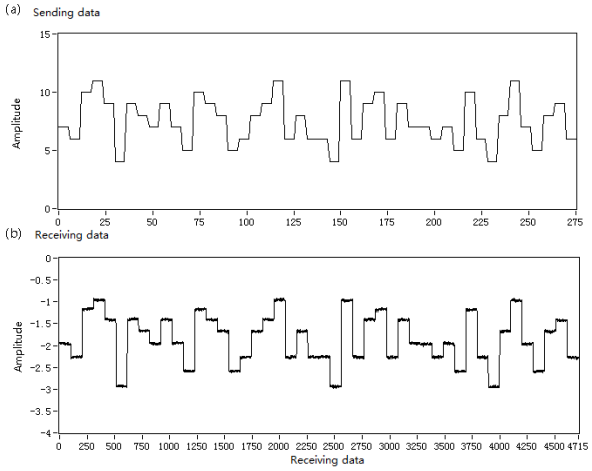

FIGURE 8. Sending and receiving data when the light power is 1 mW.

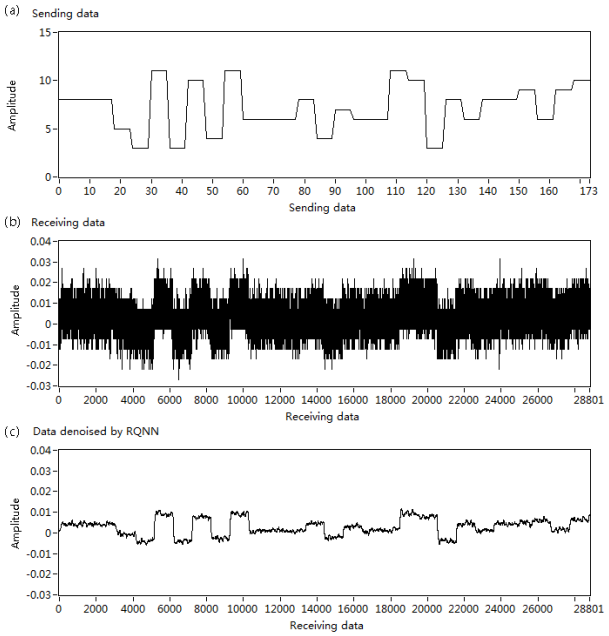

FIGURE 9. Sending, receiving and RQNN-restored data when the light power is 0.01 mW.

receiving data, bit error rate (BER) was calculated. The BER was less than 10^{-3} when the light power was 1 mW.

Then the VOA was used to attenuated the incident light power to 0.01 mW. Other experiment condition was the same as above: S_2 was selected as signal and S_3 was selected as LO at Alice's side. At Bob's side, S_2 was selected as measurement base. 16-bit Gaussian random number was used as modulating signal for S_2. Driving voltage of the multiplexer and demultiplexer was calculated and added to the devices via driving and controlling system. The sending and receiving signal are shown in Figure 9. The receiving data was embedded with heavy noise, adjacent state could hardly be separated. At this time, RQNN approach was applied for signal restoration of the receiving signal [33]. And the signal after RQNN is shown in Figure 9c. The signal-to-noise ratio was greatly enhanced after signal restoration by RQNN. After quantization of the RQNN-restored data, BER was calculated. The BER was less than 4% when the light power was 0.01 mW.

C. DISCUSSIONS

Most of the CV-QKD were conducted while splitting signal and LO as Mach-Zehnder interferometer's two arms [15]–[17]. Atmospheric scattering adds difficulty to synchronization in free space for the two beams, and it's also hard for an accurate interference of them at Bob's side. Although Huang *et al.* proposed a locally LO scheme [18], [19], it still required precise secure phase compensation. In this study, we present a multiplexing technique based on SO(3) transformation. Through this technique, two of the three Stokes parameters of the same beam, namely S_2 and S_3 is selected as signal and LO, which are from the same light beam and transmits in the same spatial mode. In other words, signal and LO are multiplexed in the same light path, which overcomes difficulties of synchronization. In addition, atmospheric turbulence has the same influence on both signal and LO, making polarization compensation more convenient.

Elser *et al.* presented an EOM and MOM joint modulation for multiplexing of coherent polarization states [21], where MOM generated a weak signal in S_2 component and EOM modulated S_3 component. Heim *et al.* improved Elser's system by using two EOMs associated with an HWP to implement polarization encoding [22], [23]. All the above schemes used discrete devices. While in this paper, three SO(3) sub-matrices were applied for the description of polarization state transformation, and a multiplexer with three $LiNbO_3$ crystals was designed. The multiplexer is an integrated device with driving and controlling system, and could achieve multiplexing of coherent polarization states.

V. CONCLUSION

In this paper, three-dimensional rotation group SO(3) was introduced to describe the transformation of coherent polarization states. Three SO(3) matrices were applied to modulate polarization states and to multiplex signal and LO. A multiplexer was designed using three anisotropic $LiNbO_3$ crystals. Combined with SO(3) matrix and Poincaré Sphere, principle of polarization multiplexing was given. The multiplexer was tested under different intensities of light. Bit error rate was less than 4% under different light intensities. Meanwhile, signal and LO transmitted in single spatial mode, multiplexing of coherent polarization states was realized. And besides application in CV-QKD, the self-made multiplexer could be served as polarization encoder or multiplexer in other optical communication systems and quantum communication systems as well.

REFERENCES

[1] B. C. Jacobs and J. D. Franson, "Quantum cryptography in free space," *Opt. Lett.*, vol. 21, no. 22, pp. 1854–1856, 1996.
[2] Y.-G. Tan, "Quantum key distribution with prepare-and-measure bell test," *Sci. Rep.*, vol. 6, no. 1, p. 35032, Dec. 2016.
[3] C.-H. Zhang, C.-M. Zhang, G.-C. Guo, and Q. Wang, "Biased three-intensity decoy-state scheme on the measurement-device-independent quantum key distribution using heralded single-photon sources," *Opt. Express*, vol. 26, no. 4, p. 4219, 2018.
[4] P. J. Coles, E. M. Metodiev, and N. Lütkenhaus, "Numerical approach for unstructured quantum key distribution," *Nature Commun.*, vol. 7, no. 1, p. 11712, Sep. 2016.
[5] H. Mao, Q. Li, Q. Han, and H. Guo, "High-throughput and low-cost LDPC reconciliation for quantum key distribution," *Quantum Inf. Process.*, vol. 18, no. 7, p. 232, Jul. 2019.
[6] K. Sedziak, M. Lasota, and P. Kolenderski, "Reducing detection noise of a photon pair in a dispersive medium by controlling its spectral entanglement," *Optica*, vol. 4, no. 1, p. 84, Jan. 2017.
[7] X. Yang, M.-Q. Bai, Z.-C. Zuo, and Z.-W. Mo, "Secure simultaneous dense coding using χ-type entangled state," *Quantum Inf. Process.*, vol. 17, no. 10, p. 261, Oct. 2018.
[8] K. Wang, X.-T. Yu, and Z.-C. Zhang, "Two-qubit entangled state teleportation via optimal POVM and partially entangled GHZ state," *Frontiers Phys.*, vol. 13, no. 5, Oct. 2018.

[9] T. Wang, P. Huang, Y. Zhou, W. Liu, H. Ma, S. Wang, and G. Zeng, "High key rate continuous-variable quantum key distribution with a real local oscillator," *Opt. Express*, vol. 26, no. 3, p. 2794, 2018.
[10] Z. Qu and I. B. Djordjevic, "High-speed free-space optical continuous-variable quantum key distribution enabled by three-dimensional multiplexing," *Opt. Express*, vol. 25, no. 7, p. 7919, 2017.
[11] R. Kumar, H. Qin, and R. Alléaume, "Coexistence of continuous variable QKD with intense DWDM classical channels," *New J. Phys.*, vol. 17, no. 4, Apr. 2015, Art. no. 043027.
[12] F. Grosshans, G. V. Assche, J. Wenger, R. Brouri, N. J. Cerf, and P. Grangier, "Quantum key distribution using Gaussian-modulated coherent states," *Nature*, vol. 421, no. 6920, pp. 238–241, 2003.
[13] L. S. Madsen, V. C. Usenko, M. Lassen, R. Filip, and U. L. Andersen, "Continuous variable quantum key distribution with modulated entangled states," *Nature Commun.*, vol. 3, no. 1, p. 1083, Jan. 2012.
[14] E. Diamanti and A. Leverrier, "Distributing secret keys with quantum continuous variables: Principle, security and implementations," *Entropy*, vol. 17, no. 12, pp. 6072–6092, Aug. 2015.
[15] Y. Liu, J. Lu, and L. Zhou, "Information gain versus interference in Bohr's principle of complementarity," *Opt. Express*, vol. 25, no. 1, p. 202, Jan. 2017.
[16] P. Jouguet, S. Kunz-Jacques, A. Leverrier, P. Grangier, and E. Diamanti, "Experimental demonstration of long-distance continuous-variable quantum key distribution," *Nature Photon.*, vol. 7, no. 5, pp. 378–381, May 2013.
[17] P. Jouguet, S. Kunz-Jacques, and T. Debuisschert, "Field test of classical symmetric encryption with continuous variables quantum key distribution," *Opt. Express*, vol. 20, no. 13, pp. 14030–14041, 2012.
[18] D. Huang, P. Huang, D. Lin, C. Wang, and G. Zeng, "High-speed continuous-variable quantum key distribution without sending a local oscillator," *Opt. Lett.*, vol. 40, no. 16, pp. 3695–3698, Aug. 2015.
[19] D. Huang, D. K. Lin, P. Huang, C. Wang, W. Q. Liu, S. H. Fang, and G. H. Zeng, "Continuous-variable quantum key distribution with 1 Mbps secure key rate," *Opt. Express*, vol. 23, no. 13, pp. 17511–17519, 2015.
[20] S. Lorenz, N. Korolkova, and G. Leuchs, "Continuous-variable quantum key distribution using polarization encoding and post selection," *Appl. Phys. B, Lasers Opt.*, vol. 79, no. 3, pp. 273–277, Aug. 2004.
[21] D. Elser, T. Bartley, B. Heim, C. Wittmann, D. Sych, and G. Leuchs, "Feasibility of free space quantum key distribution with coherent polarization states," *New J. Phys.*, vol. 11, no. 4, Apr. 2009, Art. no. 045014.
[22] B. Heim, C. Peuntinger, N. Killoran, I. Khan, C. Wittmann, C. Marquardt, and G. Leuchs, "Atmospheric continuous-variable quantum communication," *New J. Phys.*, vol. 16, no. 11, Nov. 2014, Art. no. 113018.
[23] B. Heim, D. Elser, T. Bartley, M. Sabuncu, C. Wittmann, D. Sych, C. Marquardt, and G. Leuchs, "Atmospheric channel characteristics for quantum communication with continuous polarization variables," *Appl. Phys. B, Lasers Opt.*, vol. 98, no. 4, pp. 635–640, Mar. 2010.
[24] P. Hockett, M. Wollenhaupt, C. Lux, and T. Baumert, "Complete photoionization experiments via ultrafast coherent control with polarization multiplexing. II. Numerics and analysis methodologies," *Phys. Rev. A, Gen. Phys.*, vol. 92, no. 1, Jul. 2015, Art. no. 013411.
[25] F. Grassi, J. Mora, B. Ortega, and J. Capmany, "Centralized light-source optical access network based on polarization multiplexing," *Opt. Express*, vol. 18, no. 5, pp. 4240–4245, Feb. 2010.
[26] C. Wan, J. Chen, and Q. Zhan, "Tailoring optical orbital angular momentum spectrum with spiral complex field modulation," *Opt. Express*, vol. 25, no. 13, p. 15108, 2017.
[27] M. Nazarathy and A. Agmon, "Doubling direct-detection data rate by polarization multiplexing of 16-QAM without active polarization control," *Opt. Express*, vol. 21, no. 26, pp. 31998–32012, 2013.
[28] X. Dou, H. Yin, H. Yue, and Y. Jin, "Experimental demonstration of polarization-division multiplexing of chaotic laser secure communications," *Appl. Opt.*, vol. 54, no. 14, pp. 4509–4513, 2015.
[29] A. Luis, "Quantum polarization for three-dimensional fields via Stokes operators," *Phys. Rev. A, Gen. Phys.*, vol. 71, no. 2, pp. 362–368, Feb. 2005.
[30] S. Kumar, A. Bisht, G. Singh, K. Choudhary, and D. Sharma, "Implementation of wavelength selector based on electro-optic effect in Mach–Zehnder interferometers for high speed communications," *Opt. Commun.*, vol. 350, pp. 108–118, Sep. 2015.
[31] F. Chen, H. Hu, J.-H. Zhang, F. Lu, B.-R. Shi, K.-M. Wang, D.-Y. Shen, and C.-Q. Wang, "Optical waveguide in X-Cut $LiNbO_3$ crystals by MeV P^+ ion implantation with low dose," *Phys. Status Solidi A*, vol. 187, no. 2, pp. 543–548, Oct. 2001.
[32] S. Y. Lu and R. A. Chipman, "Interpretation of Mueller matrices based on polar decomposition," *J. Opt. Soc. Amer. A, Opt. Image Sci.*, vol. 13, no. 5, pp. 1106–1113, 1996.
[33] W. Lu, C. Huang, K. Hou, L. Shi, H. Zhao, Z. Li, and J. Qiu, "Recurrent neural network approach to quantum signal: Coherent state restoration for continuous-variable quantum key distribution," *Quantum Inf. Process.*, vol. 17, no. 5, p. 109, May 2018.

WEIZHAO LU was born in Tai'an, Shandong, China, in 1990. He received the B.S. degree in microelectronics from the Jiangnan University, Wuxi, in 2013, and the M.S. degree in physical engineering from Fuzhou University, Fuzhou, in 2016.

From 2016 to 2019, he was a Research Assistant with the Medical Engineering and Technology Research Center, Shandong First Medical University and Shandong Academy of Medical Sciences. He has authored more than ten articles and three inventions. His research interests include medical imaging analysis, neuroimaging, and quantum correlated imaging. He was a member of the Radiological Society of North America, in 2019.

JIANFENG QIU received the Ph.D. degree in biomedical engineering from Capital Medical University, in 2012, and the Ph.D. degree in radiological physics from the University of Washington, in 2015. From May 2014 to October 2014, he was a Visiting Scholar with the University of Washington. Till now, he has been the Director of the Medical Engineering Technology Research Center, Shandong First Medical University.

Dr. Qiu hosted the National Key Research and Development Program of China as the Chief Scientist. He has two Natural Science Foundations of Shandong Province and participated in one National Key Research and Development Plan of China. His research interests include optical imaging, quantum correlated imaging, medical imaging, and imaging physics.